# Terahertz and far infrared Spectroscopy of alanine-rich peptides having variable ellipticity

**Tao Ding,[1] Ruoyu Li,[2] J. Axel Zeitler,[2] Thomas L. Huber,[3] Lynn F. Gladden,[2] Anton P. J. Middelberg[1] and Robert J. Falconer[1*]**

[1] *Australian Institute for Bioengineering and Nanotechnology, The University of Queensland, Brisbane, Australia*
[2] *Department of Chemical Engineering and Biotechnology, The University of Cambridge, Cambridge CB2 3RA, UK*
[3] *Research School of Chemistry, Australian National University, Canberra, Australia*
** r.falconer@uq.edu.au*

**Abstract:** Terahertz spectra of four alanine-rich peptides with known secondary structures were studied by terahertz time domain spectroscopy (THz-TDS) and by Fourier transform infrared spectroscopy (FTIR) using a synchrotron light source and a liquid-helium cooled bolometer. At ambient temperatures the usable bandwidth was restricted to 0.2-1.5 THz by the absorbance of water. The existence of a solvation shell around the peptide in solution was observed and its size estimated to be between 11 and 17 Å. By cooling the peptide solution to 80 K in order to reduce the water absorbance the bandwidth was increased to 0.1-3.0 THz for both THz-TDS and FTIR. Spectra were consistent with monotonic absorbance of the peptide and the existence of a solid amorphous low density solvation shell.



**OCIS codes (**300.6495) Spectroscopy, terahertz; (170.0170) Medical optics and biotechnology.

## References and links

1. M. Walther, P. Plochocka, B. Fischer, H. Helm, and P. Uhd Jepsen, "Collective vibrational modes in biological molecules investigated by terahertz time-domain spectroscopy," Biopolymers **67**(4-5), 310–313 (2002).
2. B. Fischer, M. Hoffmann, H. Helm, G. Modjesch, and P. U. Jepsen, "Chemical recognition in terahertz time-domain spectroscopy and imaging," Semicond. Sci. Technol. **20**(7), S246–S253 (2005).
3. M. Walther, B. M. Fischer, and P. U. Jepsen, "Noncovalent intermolecular forces in polycrystalline and amorphous saccharides in the far infrared," Chem. Phys. **288**(2-3), 261–268 (2003).
4. B. Brooks, and M. Karplus, "Normal modes for specific motions of macromolecules: application to the hinge-bending mode of lysozyme," Proc. Natl. Acad. Sci. U.S.A. **82**(15), 4995–4999 (1985).
5. Y. Seno, and N. Go, "Deoxymyoglobin studied by the conformational normal mode analysis. II. The conformational change upon oxygenation," J. Mol. Biol. **216**(1), 111–126 (1990).
6. W. N. Wang, Y. B. Li, and W. W. Yue, "Vibrational spectrum of histidine and arginine in THz range," Acta. Phys. Sin. **56**, 781–785 (2007).
7. R. Rungsawang, Y. Ueno, I. Tomita, and K. Ajito, "Angle-dependent terahertz time-domain spectroscopy of amino acid single crystals," J. Phys. Chem. B **110**(42), 21259–21263 (2006).
8. A. G. Markelz, A. Roitberg, and E. J. Heilweil, "Pulsed terahertz spectroscopy of DNA, bovine serum albumin and collagen between 0.1 and 2.0 THz," Chem. Phys. Lett. **320**(1-2), 42–48 (2000).
9. G. M. Png, R. J. Falconer, B. M. Fischer, H. A. Zakaria, S. P. Mickan, A. P. J. Middelberg, and D. Abbott, "Terahertz spectroscopic differentiation of microstructures in protein gels," Opt. Express **17**(15), 13102–13115 (2009).
10. S. Ebbinghaus, S. J. Kim, M. Heyden, X. Yu, U. Heugen, M. Gruebele, D. M. Leitner, and M. Havenith, "An extended dynamical hydration shell around proteins," Proc. Natl. Acad. Sci. U.S.A. **104**(52), 20749–20752 (2007).
11. J. Xu, K. W. Plaxco, and S. J. Allen, "Probing the collective vibrational dynamics of a protein in liquid water by terahertz absorption spectroscopy," Protein Sci. **15**(5), 1175–1181 (2006).
12. M. Nagai, H. Yada, T. Arikawa, and K. Tanaka, "Terahertz time-domain attenuated total reflection spectroscopy in water and biological solution," Int. J. Infrared Millim. Waves **27**(4), 505–515 (2007).
13. E. Castro-Camus, and M. B. Johnston, "Conformational changes of photoactive yellow protein monitored by terahertz spectroscopy," Chem. Phys. Lett. **455**(4-6), 289–292 (2008).
14. Y. F. He, P. I. Ku, J. R. Knab, J. Y. Chen, and A. G. Markelz, "Protein dynamical transition does not require protein structure," Phys. Rev. Lett. **101**(17), 178103 (2008).
15. A. G. Markelz, J. R. Knab, J. Y. Chen, and Y. F. He, "Protein dynamical transition in terahertz dielectric response," Chem. Phys. Lett. **442**(4-6), 413–417 (2007).

#137135 - $15.00 USD Received 27 Oct 2010; revised 8 Dec 2010; accepted 8 Dec 2010; published 14 Dec 2010

16. B. Born, H. Weingärtner, E. Bründermann, M. Havenith, "Solvation dynamics of model peptides probed by terahertz spectroscopy. Observation of the onset of collective network motions Observation of the Onset of Collective Network Motions," J. Am. Chem. Soc. **131**(10), 3752–3755 (2009).
17. A. Chakrabartty, T. Kortemme, and R. L. Baldwin, "Helix propensities of the amino acids measured in alanine-based peptides without helix-stabilizing side-chain interactions," Protein Sci. **3**(5), 843–852 (1994).
18. T. Hirschfeld, and A. W. Mantz, "Elimination of thin-film infrared channel spectra in fourier-transform infrared spectroscopy," Appl. Spectrosc. **30**(5), 552–553 (1976).
19. E. Lindahl, B. Hess, and D. van der Spoel, "GROMACS 3.0: a package for molecular simulation and trajectory analysis," J. Mol. Model. **7**, 306–317 (2001).
20. B. Born, S. J. Kim, S. Ebbinghaus, M. Gruebele, and M. Havenith, "The terahertz dance of water with the proteins: the effect of protein flexibility on the dynamical hydration shell of ubiquitin," Faraday Discuss. **141**, 161–173, discussion 175–207 (2008).
21. T. Arikawa, M. Nagai, and K. Tanaka, "Characterizing hydration state in solution using terahertz time-domain attenuated total reflection spectroscopy," Chem. Phys. Lett. **457**(1-3), 12–17 (2008).
22. S. Mashimo, S. Kuwabara, S. Yagihara, and K. Higasi, "Dielectric-releaxation time and structure of bound water in biological materials," J. Phys. Chem. **91**(25), 6337–6338 (1987).
23. P. M. Chaikin, A. Donev, and W. Man, F. H. Stillinger and S. Torquato, "Some observations on the random packing of hard ellipoiods," Ind. Eng. Chem. Res. **45**, 6960–6965 (2006).
24. U. Heugen, G. Schwaab, E. Bründermann, M. Heyden, X. Yu, D. M. Leitner, and M. Havenith, "Solute-induced retardation of water dynamics probed directly by terahertz spectroscopy," Proc. Natl. Acad. Sci. U.S.A. **103**(33), 12301–12306 (2006).
25. J. E. Bertie, H. J. Labbe, and E. Whally, "Absorptivity of ice I in range 4000-30 cm-1," J. Chem. Phys. **50**(10), 4501–4520 (1969).
26. G. W. Chantry, E. A. Nicol, H. A. Willis, and M. E. A. Cudby, "Far infrared studies of the formation of potassium fluoride dihydrate in and its interaction with low molecular weight polytetrafluorethylene," Int. J. Infrared Millim. Waves **2**(1), 97–105 (1981).
27. C. J. Raj, S. Krishnan, S. Dinakaran, R. Uthrakumar, and S. J. Das, "Growth and optical absorption studies on potassium dihydrogen phosphate single crystals," Cryst. Res. Technol. **43**(3), 245–247 (2008).
28. A. H. Xie, Q. He, L. Miller, B. Sclavi, and M. R. Chance, "Low frequency vibrations of amino acid homopolymers observed by synchrotron far-IR absorption spectroscopy: Excited state effects dominate the temperature dependence of the spectra," Biopolymers **49**(7), 591–603 (1999).
29. A. K. Soper, "Structural transformations in amorphous ice and supercooled water and their relevance to the phase diagram of water," Mol. Phys. **106**(16), 2053–2076 (2008).
30. S. H. Chen, L. Liu, E. Fratini, P. Baglioni, A. Faraone, and E. Mamontov, "Observation of fragile-to-strong dynamic crossover in protein hydration water," Proc. Natl. Acad. Sci. U.S.A. **103**(24), 9012–9016 (2006).
31. J. A. Zeitler, P. F. Taday, K. C. Gordon, M. Pepper, and T. Rades, "Solid-state transition mechanism in carbamazepine polymorphs by time-resolved terahertz spectroscopy," ChemPhysChem **8**(13), 1924–1927 (2007).
32. J. A. Zeitler, P. F. Taday, M. Pepper, and T. Rades, "Relaxation and crystallization of amorphous carbamazepine studied by terahertz pulsed spectroscopy," J. Pharm. Sci. **96**(10), 2703–2709 (2007).
33. S. C. Shen, L. Santo, and L. Genzel, "THz spectra for some bio-molecules," Int. J. Infrared Millim. Waves **28**(8), 595–610 (2007).
34. F. Haselhuhn, S. Doyle, and M. Kind, "Synchrotron radiation X-ray diffraction study of the particle formation of pseudo-polymorphic calcium oxalate," J. Cryst. Growth **289**(2), 727–733 (2006).
35. I. Jelesarov, E. Dürr, R. M. Thomas, and H. R. Bosshard, "Salt effects on hydrophobic interaction and charge screening in the folding of a negatively charged peptide to a coiled coil (leucine zipper)," Biochemistry **37**(20), 7539–7550 (1998).
36. G. H. Nancollas, and G. L. Gardner, "Kinetics of crystal-growth of calcium-oxalate monohydrate," J. Cryst. Growth **21**(2), 267–276 (1974).
37. R. J. Falconer, H. A. Zakaria, Y. Y. Fan, A. P. Bradley, and A. P. J. Middelberg, "Far-infrared spectroscopy of protein higher-order structures," Appl. Spectrosc. **64**(11), 1259–1264 (2010).

## 1. Introduction

There is ongoing interest in developing analytical techniques that provide information pertaining to the structure of macromolecules such as proteins. The measurement of long-range low-energy molecular motions within a macromolecule provides a potential route to structural understanding. The advent of terahertz time-domain spectroscopy (THz-TDS) provides an opportunity to study the absorbance of low-energy photons [1]. THz-TDS has been proven to be effective at the recognition of organic and inorganic crystals which display strong intermolecular modes at discrete frequencies, reported as phonon-like resonances [2,3]. The application of THz-TDS to biomacromolecules has been limited, and there is scope to better understand their behavior in this part of the spectrum. Early theoretical studies have predicted that proteins have vibrational resonance in the far infrared frequency range [4,5].

#137135 - $15.00 USD Received 27 Oct 2010; revised 8 Dec 2010; accepted 8 Dec 2010; published 14 Dec 2010

Recently, there is increasing interest in applying THz-TDS to biological samples. Examples of the materials studied include amino acids [6,7], proteins in solution [8], protein in a gel state [9] and the solvation shell around protein molecules [10]. While this is a promising approach from a spectroscopic perspective, studies in this field have been limited by the lack of benchmark spectra and restricted by the absorbance properties of water that occur across part of THz-TDS range.

Recent studies of proteins in an aqueous environment at terahertz frequencies can be broadly divided into two categories: studies carried out at room temperatures [11–13] and investigations of frozen samples with reduced background absorption due to bulk water in the sample [14,15]. In addition to THz-TDS and Fourier transform infrared spectroscopy (FTIR) it is also possible to use a high power terahertz source such as a p-Ge laser to study samples at specific frequencies in the range of 2.1-2.8 THz [16]. By analyzing the nonlinear relationship between solute concentration and the terahertz absorption, this technique provides insight into the interaction between proteins and water, as allowing investigation of so-called biological water or the solvation shell. In THz-TDS studies of frozen protein samples, ice exhibits a low absorbance below 2 THz. By using a high protein concentration (up to 40% by weight) a protein spectrum can be acquired over the range of 0.2-2.0 THz. Through variable temperature measurements researchers were able to detect a so-called protein dynamical transition at around 200 K [14]. The transition is thought to be due to a change in rigidity of the biological water that constrains the motion of the protein molecule.

In this study we analyzed a series of peptides. Peptides are polymers of amino acids and are small versions of proteins. They have the advantage that relatively easily defined structures can be built into their design. We used three synthesized alanine-based peptides [17] which were chemically very similar but differ considerably in their secondary structure (Table 1). The peptide AK17 has an alpha helical (spiral) structure, which was reduced in AK10G and nearly eliminated in AK9P. A THz-TD spectrometer was used to measure each peptide sample in solution at both room temperature and at 79 ± 1 K. In addition, a FTIR spectrometer with a liquid-helium-cooled bolometer and a synchrotron light source was used to verify the THz-TD data. The aim of this work is to contribute understanding on sample preparation for analysis in the terahertz range, and open up the method for detection of protein structural elements of proteins and peptides in the terahertz domain.

## 2. Experimental details

### *2.1 Sample preparation*

Three alanine-rich peptides were chemically synthesized with higher than 95% purity (Mimotopes, Clayton, Australia). The amino acid sequences of these three peptides (AK17, AK10G and AK9P) are provided in Table 1. AK17 is an alanine-rich peptide made from seventeen amino acids with four lysine residues. AK10G differed from AK17 by one glycine residue that was substituted at the 10th position. AK9P differed from AK17 by one proline residue that was substituted at the 9th position. In addition, a peptide named AQ17 was synthesized with purity higher than 95% (Genscript, Piscataway, NJ, USA). AQ17 was an alanine-based peptide made from seventeen amino acids with four glutamine residues (Table1). Two solutions were used in this study: a) 100 mM potassium fluoride 1 mM potassium phosphate buffer, pH7 (KF buffer); b) 10 mM phosphate buffer, pH 7.4 (Phosphate buffer). The secondary structures of the peptides were measured by circular dichroism spectroscopy using KF buffer and the percentage of helicity was estimated from the $\theta_{222}$ value (Table 1). The peptide was dissolved in buffer for spectroscopic measurement, at concentrations between 3.125 mM and 50 mM.

#137135 - $15.00 USD Received 27 Oct 2010; revised 8 Dec 2010; accepted 8 Dec 2010; published 14 Dec 2010

*2.2 Terahertz time-domain spectroscopy*

Figure 1 shows a schematic plot of the terahertz time-domain spectroscopy (THz-TDS) arrangement used in experiments. A Ti:sapphire laser (Femtosource cM1, Femtolasers, Vienna, Austria: 500 mW; wavelength range: 650-950 nm) was pumped by a Millenia Xs continuous-wave laser (Spectra Physics: Mountain View, USA, 6 W output power, 532 nm) to produce 12 fs laser pulses centred at approximately 800 nm (bandwidth >100 nm) at a repetition rate of 80 MHz. This laser beam was split into a pump beam (99% power) and a probe beam (1% power) that were used to generate and detect terahertz radiation, respectively. The pump beam was focused onto a DC-biased semi-insulating LT-GaAs emitter to generate sub-picosecond coherent pulses of broadband terahertz radiation (0.1 – 4.0 THz, 3-133 $cm^{-1}$) by photoexcitation. The terahertz beam reflected from the emitter surface was then collimated and focused onto the sample using a pair of parabolic mirrors. The transmitted terahertz signal was detected via electrooptic sampling using a ZnTe crystal. Time-domain spectra were collected by employing a 50 ps optical delay, oscillating at a frequency of 0.5 Hz.

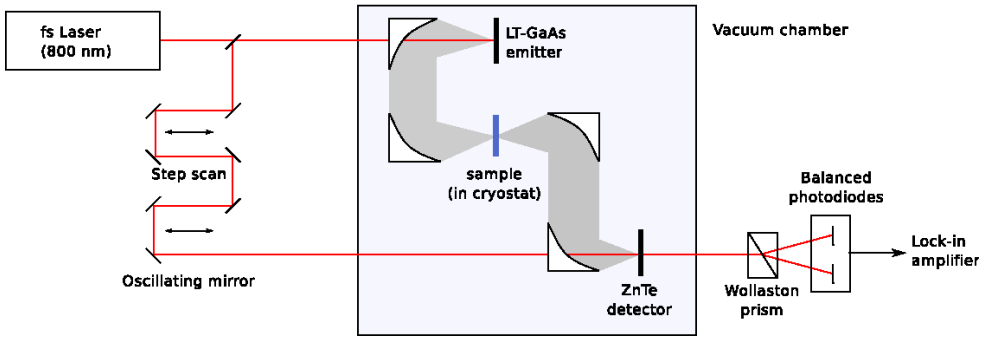


Fig. 1. The terahertz time-domain spectroscopy (THz-TDS) arrangement.

To control the sample temperature, a custom made copper cold finger was fitted to a modified continuous flow cryostat (Janis ST-FTIR, Berkeley, CA, USA). The shroud of the cryostat was removed and the cold finger was fitted directly into the sample compartment, which was evacuated to 15 mbar (PT70 F-Compact, Oerlikon-Leybold, Cologne, Germany). The cold finger was fitted with three holes of 8 mm diameter each. To hold the liquid sample a PE window and a 270 µm thick spacer were mounted onto the cold finger. 16 µl liquid sample was placed between the two PE windows and spread while tightening the windows between the spacer using screws and a further plate of copper with an aperture. Excess liquid was wiped off after filling the sample cells. The cryostat was then fitted into the sample compartment, the sample compartment was evacuated and using an evacuated transfer tube the cryostat was connected with a liquid nitrogen Dewar. The cooling rate of the cold finger was adjusted by controlling the flow of nitrogen into the transfer tube, and in turn the pressure of nitrogen in the Dewar, by a needle valve. Samples were cooled to 79 ± 1 K and then heated to room temperature. Spectra were acquired after an equilibration time of 15 min. For each run one peptide sample, a reference buffer sample without peptide and an empty cell without spacer were mounted on the cold finger. The temperature of the cold finger was controlled using a temperature controller (331S, Lake Shore, Westerville, OH, USA). Using a motorized stage it was possible to swap between the different samples during the experiment and time-domain waveforms were acquired for all samples. For each measurement, 200 time-domain waveforms were collected, averaged and then transformed into the frequency domain by fast Fourier transform (FFT). A cut-off time of 20 ~40 ps was used for the FFT to prevent etalon artifacts due to multiple reflections, resulting in a spectral resolution of about 30 GHz (1 $cm^{-1}$).

#137135 - $15.00 USD Received 27 Oct 2010; revised 8 Dec 2010; accepted 8 Dec 2010; published 14 Dec 2010

*2.3 Far infrared Spectroscopy using a Synchrotron Light Source*

Far infrared Spectroscopic measurements were performed on the far infrared and high resolution FTIR beamline at the Australian Synchrotron (Clayton, Victoria) operating at 3 GeV and a maximum current of 200 mA. The beam dimension was 480 micron (horizontal) by 13 micron (vertical), the opening angle collected was 50 mrad (horizontal) by 16 mrad (vertical). The beam was a converging source close to a point. 16 µl liquid sample was placed between the two polypropylene (PP) windows and spread while tightening the windows between the spacer using screws and a further plate of copper with an aperture. To hold the liquid sample a PP window and a 270 µm thick spacer were mounted onto the cold finger. The sample was mounted in a Janis ST-100FTIR cryostat (Wilmington, MA, USA) with a similar cold finger configuration to that used for the THz-TDS analysis and cooled with liquid nitrogen to 78 K. The temperature of the cold finger was measured using a temperature controller (331S, Lake Shore, Westerville, OH, USA). Transmission spectra were recorded using the Bruker IFS 125HR Fourier Transform Infrared spectrometer (Bruker Optics, Ettlingen, Germany) fitted with a 6 µm Mylar multilayer beam splitter, scanner velocity of 40 kHz, and a liquid helium-cooled Si bolometer detector with aperture setting of 4 mm. Each spectrum was an average of 26 scans recorded with the maximum frequency limit of 21.0 THz (700 $cm^{-1}$) and at a resolution of 7.5 GHz (0.25 $cm^{-1}$). To eliminate the etalon effect due to reflection of the measurement cell, a Tukey window with apodisation function [18] was applied to all interferograms prior to FFT.

*2.4 Computer modeling for excluded volume of peptide*

The solvent excluded volume is the volume of space from which solvent molecule is excluded by the presence of the biomolecules. To model the excluded volume of each peptide molecule, classical molecular dynamics simulations were performed with the GROMACS 3.3.2 software [19]. The AK17, AK10G and AK9P molecules were initially modeled as alpha helix conformations by restricting the Phi and Psi angles. These peptides were dissolved in a simulation box of 1.2 nm in each dimension and the SPC (single point charge, 3-point) water model was used. GROMOS 45A3 force field was used and 6 ns of simulation were performed under NPT conditions (number of particles ($N$), system pressure ($P$) and temperature ($T$) held constant) for each peptide. Energy minimization was performed on the peptides using a steepest-descent algorithm with a tolerance of 0.01. The time evolution of their momentary positions and velocities (the trajectory) were calculated by iteratively integrating Newton's equations of motion. The conformation was determined at the end of the simulation and the water exclusion was then determined [17]. For each peptide molecule, the radius of gyration ($R_g$) was estimated in GROMACS, the excluded water volume ($V_{excluded}$) per peptide molecule was then calculated according to Eq. (1).

$$V_{excluded} = \frac{4}{3}\pi(\sqrt{5/3}R_g)^3 \tag{1}$$

The proportion of water excluded ($P_{excluded}$) in a solution with given concentration was then calculated using Eq. (2).

$$P_{excluded} = \frac{N_{solute}V_{excluded}}{V_{solution}} \tag{2}$$

where $N_{solute}$ is the number of peptide molecules within a solution volume ($V_{solution}$).

According to Beer-Lambert's law, absorbance is directly proportional to the thickness of the sample. The absorbance of the sample that is corrected to take the excluded volume into account ($A_{excluded}$) is calculated from the absorbance of the buffer ($A_{buffer}$) by Eq. (3).

#137135 - $15.00 USD Received 27 Oct 2010; revised 8 Dec 2010; accepted 8 Dec 2010; published 14 Dec 2010

$$A_{excluded} = A_{buffer}(1 - P_{excluded}) \quad (3)$$

*2.5 Estimating the thickness of the solvation shell*

The genbox program in GROMACS 3.3.2 software was also used to estimate the thickness of the peptide solvation shell. The conformation of the three peptides at the end of the simulation used to estimate $V_{excluded}$ was used as an initial condition. To estimate the thickness of the solvation shell, the number of water molecules per peptide molecule was estimated for the peptide concentration at the point of inflection in the graph of relative absorbance versus peptide concentration. By thus constraining the thickness of the water layer in each dimension, SPC water was placed around a peptide molecule with no bias and the water layers corresponding to each peptide concentration were constructed and the apparent thickness of the solvation shell obtained.

*2.6 Calculating the average relative absorbance at 0.2-1.5 THz*

Each room temperature THz-TDS spectrum comprised 59 data points in the frequency range of 0.2-1.5 THz. The data points were used to calculate the average relative absorbance $A_r$, according to Eq. (4), where $A_{sample}$ and $A_{buffer}$ are the absorbance of sample and buffer at a given frequency, respectively.

$$A_r = \frac{\sum_{i=1}^{N=59} \left( (A_{sample})_i / (A_{buffer})_i \right)}{N} \quad (4)$$

## 3. Results and discussion

*3.1 Room temperature measurement*

THz-TDS measurements were performed for the three alanine-rich peptides (AK17, AK10G and AK9P). The peptides were dissolved in KF buffer at concentrations of 12.5 mM, 25 mM and 50 mM and the measurements were carried out at room temperature (293 K). Due to the strong absorbance of water in this frequency range, the bandwidth of the resulting spectra was restricted to 0.2-1.5 THz. For all three peptides we observed a monotonic increase in absorbance with increasing frequency. No distinct absorption bands were observed (Fig. 2). Absorbance across the whole spectral range was lower for the samples with buffer containing peptide than for the blank buffer samples. This was consistent for all samples tested and can be explained by volume exclusion of water molecules by the peptide molecules. The peptide molecules displace the more strongly absorbing water molecules and hence a lower overall absorbance is observed. The volume exclusion effect of the peptides was simulated using molecular modeling. In a two-component scenario (neglecting biological water), where only peptide and bulk water are considered, the volume excluded by solute was estimated by calculating the surface radius per peptide molecule [20] (Table 1). The absorbance of this excluded volume model was calculated using Eqs. (2) and 3. The calculated effect of volume exclusion on absorbance is shown as the black dotted line in Fig. 2. The experimentally-measured absorbance of the peptide solution was consistently lower than that of buffer, even after correcting for peptide volume exclusion as outlined above. This finding indicates that the observed reduction in total absorbance due to the presence of the peptide cannot be fully explained only by the volume exclusion effect.

#137135 - $15.00 USD Received 27 Oct 2010; revised 8 Dec 2010; accepted 8 Dec 2010; published 14 Dec 2010

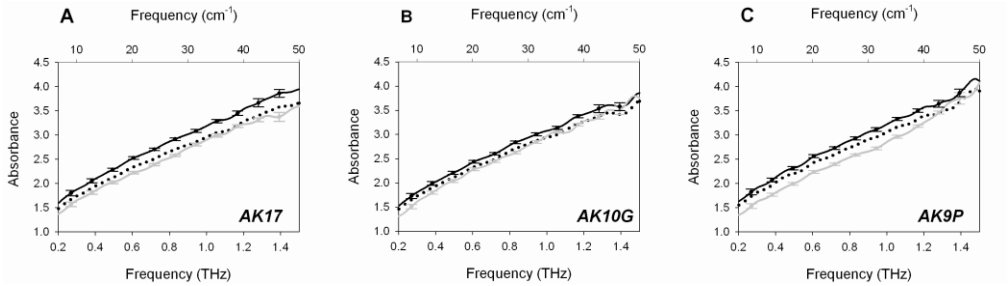


Fig. 2. THz-TDS measurements of peptide samples at room temperature. A) 25 mM AK17 B) 25 mM AK10G and C) 25 mM AK9P in 0.1 M KF solution, windows of the measuring cell are used as the reference. The respective buffer absorption is also shown in black and the peptide solution absorption shown in grey. The black dot line estimated absorption of buffer considering the volume exclusion effect exerted by the peptide. The error bars represent instrument error.

To further investigate this effect the mean absorbance in the range of 0.2-1.5 THz was calculated using Eq. (4), normalized to buffer and plotted over the entire concentration range (Fig. 3). This was undertaken for both experimental results and the results calculated using the excluded volume model. The excluded volume model predicted a linear decrease in mean absorbance with increasing peptide concentration (Fig. 3). This was in contrast to the experimental results where the strong initial decrease in absorbance was followed by a plateau commencing at 25 mM for AK17 and AK9P, and at 12.5 mM for AK10G). At the highest peptide concentration of 50 mM, both the experimental and the predicted absorbance are in agreement. We concluded that the volume exclusion effect can largely explain the decrease in absorbance at 50 mM peptide concentration. At lower peptide concentrations, the volume exclusion effect was less dominant, and bulk water was present in addition to the water molecules that form the peptide's solvation shell. The initial decrease in absorbance is thus a combination of two effects, the volume exclusion of the peptide and the solvation shell associated with the peptide, which has different absorbance compared to bulk water. Similar absorbance change attributed to the biological water around protein molecules has been recently reported elsewhere [10,20]. Arikawa *et al.* reported a lower absorption coefficient for biological water around a sugar molecule compared to bulk water, using terahertz attenuated total reflection spectroscopy [21]. Mashimo *et al.* used time-domain reflectometry to observe the relaxation motion of water in a solvation shell occurred on a time scale of nanoseconds or microseconds [22], which was much slower than the relaxation motion of bulk water (approx. 8 picoseconds orientational relaxation time). Our observation at around 1 THz of a decreased absorbance due to an increase in the biological water population agrees with these previous studies.

#137135 - $15.00 USD Received 27 Oct 2010; revised 8 Dec 2010; accepted 8 Dec 2010; published 14 Dec 2010

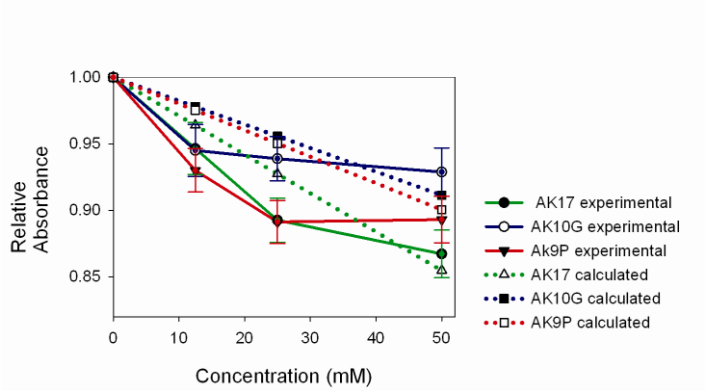


Fig. 3. Room temperature THz-TDS measurements of peptide solution absorbance relative to KF buffer. Data points from 0.2 to 1.5 THz were used. The experimental result are shown as solid lines and the modelling result are shown as dot lines. AK17 (green), AK10G (blue) and AK9P (red). The error bars represent instrument error.

As the peptide concentration was increased it was possible to observe a slower rate of decrease in absorbance, which suggests the onset of overlap in the peptide solvation shells. We propose that the solvation shells of the peptide molecules start to significantly overlap at 25 mM peptide concentration for AK17 and AK9P, and at 12.5 mM for AK10G, consistent with the observed plateau onset. Using computational modeling described in the methods section, we determined the apparent solvation shell thickness to be between 10.8, 17.3 and 11.2 Å for the peptides AK17, AK10G and AK9P (Table 1). Figure 4 illustrates that the three peptides adopt stable conformations after 5 ns of simulation. The final conformations showed that AK10G had a structure that was more spherical than AK17 and AK9P, which were more ellipsoid, consistent with AK17 having the lowest radius of gyration (Table 1). The packing density of spherical objects is lower than that of ellipsoid objects [23] which may in part account for differences in the apparent solvation shell thicknesses. The apparent solvation shell thickness of the peptides are bound by the approx. 5 Å value proposed for a carbohydrate molecule [24] and 20 Å suggested for a protein molecule [10]. While our results were dependent on the errors associated with the estimation of the point of inflection in the THz-TDS measurements of peptide solution absorbance versus concentration to indicated overlap of the solvation shells they do demonstrate that peptide-water interactions can be studied at terahertz frequencies at room temperature.

**Table 1. The four peptide's amino acid sequence, helicity (from literature and measured by circular dichroism spectroscopy), radius of gyration (calculated) and apparent solvation shell thickness (experimental).**

| Name | Amino acid Sequence | Helicity (Ref 17) | Helicity (measured) | Peptide radius of gyration * | Apparent solvation shell thickness** |
|---|---|---|---|---|---|
| AK17 | ACAKAAAAKAAAAKAA AAK-$NH_2$ | 67.7% | 72.4% | 10.5 Å | 10.8 Å |
| AK10G | ACAKAAAAKAAGAKAA AAK-$NH_2$ | 25.6% | 29.5% | 8.9 Å | 17.3 Å |
| AK9P | ACAKAAAAKAPAAKAAA AK-$NH_2$ | 0.0 | 0.0 | 9.2 Å | 11.2 Å |
| AQ17 | ACAQAAAAQAAAAQAA AAQ-$NH_2$ | NA | NA | NA | NA |

* Calculated from the excluded volume as described in method section.

**The method for calculating the apparent thickness of water around a peptide molecule from the experimental data assuming the inflection point for AK17 and AK9P is 25 mM, and AK10G is 12.5 mM (see Fig. 3).

#137135 - $15.00 USD Received 27 Oct 2010; revised 8 Dec 2010; accepted 8 Dec 2010; published 14 Dec 2010

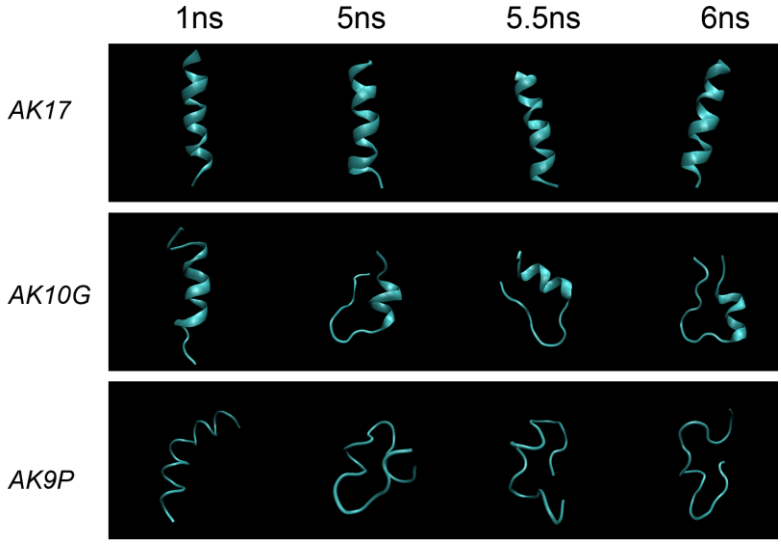


Fig. 4. Peptide (AK17, AK10G and AK9P) conformation at 1, 5, 5.5 and 6 ns of simulation by Gromacs software showing differences in peptide conformation and structural stabilization after 5 ns of simulation.

### *3.2 Low temperature measurement using a THz-TDS and a FTIR setup*

In an attempt to directly measure the dielectric properties of peptide molecules in an aqueous environment, we cooled the samples using liquid nitrogen to 79 ± 1 K. At 79 K the absorbance of water was much lower than at room temperature and hence a usable spectral bandwidth of 0.1-3 THz was achieved using the same THz-TDS spectrometer. The low overall absorbance of ice in the far infrared range was consistent with that previously reported [25]. The absorption spectra of all three peptides in KF buffer are shown in Fig. 5. We observed very low absorbance for the frequency range of 0.1-1 THz in all samples. At frequencies greater than 1 THz the absorbance spectra of peptide and buffer monotonically increased with frequency. Figure 5D outlines the concentration dependence of the three peptides, showing that at concentrations lower than 12.5 mM, a drop in absorbance relative to buffer was observed for all three peptides. In contrast to observations at room temperature, the absorbance increased monotonically with peptide concentration beyond 12.5 mM (Fig. 5D). No specific spectral features were observed for the peptide solution in buffer, while the spectra of the KF buffer exhibited absorbance peaks at 1.66, 2.32 and 2.64 THz, (shown by arrows in Fig. 6A) which are characteristic for crystalline KF dihydrate that forms in the KF buffer upon freezing [26].

In addition to the THz-TDS measurement, a FTIR spectrometer using synchrotron radiation was used to replicate the same set of measurements. Using the FTIR spectrometer a bandwidth of 1 to 15 THz could be studied, thus making this setup a very useful complementary technique to THz-TDS. However, for measurement of the samples in this study the bandwidth was restricted by a strong ice absorption peak with a maxima at approx. 7 THz, hence the resulting absorption spectra has a usable bandwidth of 1-4 THz before exceeding the dynamic range of the instrument. As shown in Fig. 6, THz-TD spectra and FTIR spectra are in good agreement, demonstrating that results from these two experimental setups were reproducible and complementary. Both methods confirmed the formation of KF dihydrate crystals in the KF buffer upon freezing of the sample. The presence of peptide inhibited the crystallization of KF dihydrate (Fig. 6), which again was also observed using both THz-TDS and FTIR. While we focused in analyzing spectra with respect to peptide-related dynamics, one should not overlook the absorption effect of KF salt crystals. To

#137135 - $15.00 USD Received 27 Oct 2010; revised 8 Dec 2010; accepted 8 Dec 2010; published 14 Dec 2010

address this issue, we substituted the KF buffer with a low concentration phosphate buffer, which does not possess measurable phonon-like resonance in the 0.1-4 THz region under our experimental conditions. This finding was further confirmed with the absence of an absorption peaks at 3.44 THz reported in previous studies [27] indicating that the phosphate salts did not crystallize as the samples were frozen. Shown in Fig. 7, the same monotonic increase in absorbance with peptide concentration was obtained and we concluded this trend was independent of the existence of salt crystals. In addition to the absorption peaks of KF dihydrate crystals identified earlier, a peak centered at 3.18 THz was observed in the FTIR measurement. Its absorption peak shifted by ~0.1 THz when water was substituted with deuterium oxide in the experiment (data not shown) providing strong evidence that this was an ice related absorption peak.

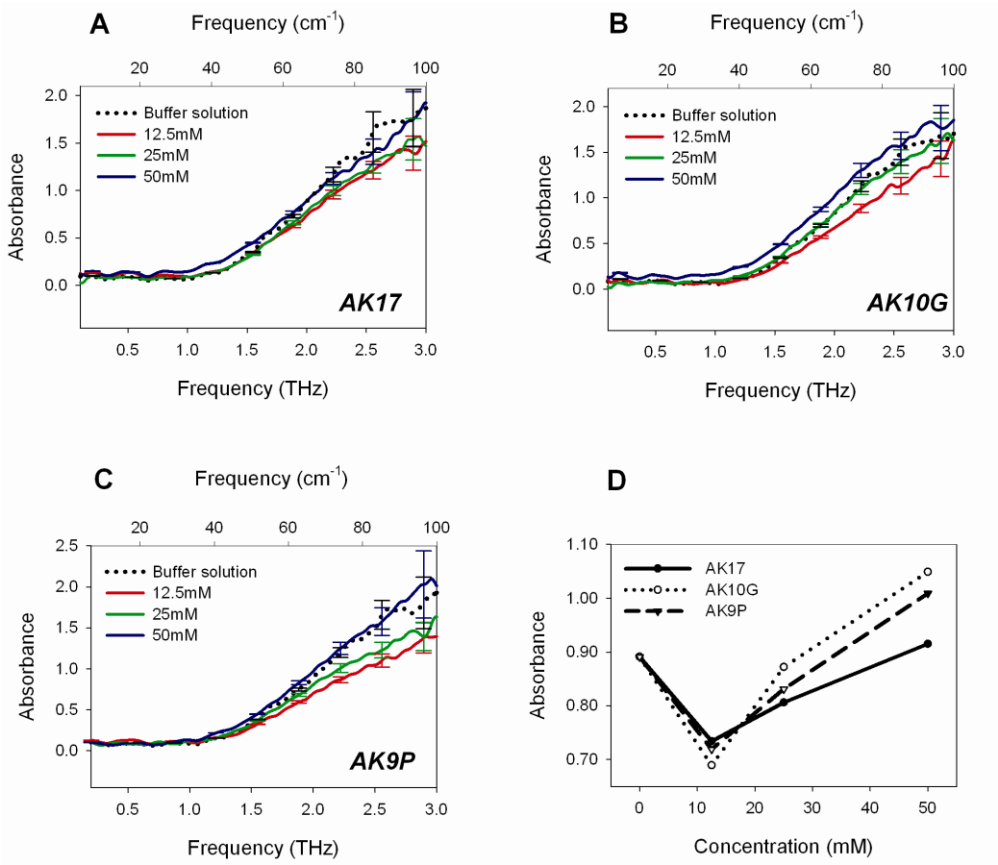


Fig. 5. THz-TDs measurements of low temperature liquid. Experiments were performed at 79 K: A) AK17 in KF buffer, B) AK10G in KF buffer, C) AK9P in KF buffer. The 50 mM sample is shown in blue, 25 mM sample is shown in green and 12.5 mM sample is shown in red. The buffer line is shown as a dot ted line. D) Concentration dependence of AK17, AK10G and AK9P, data point at 2 THz was used. The error bars represent instrument error.

#137135 - $15.00 USD Received 27 Oct 2010; revised 8 Dec 2010; accepted 8 Dec 2010; published 14 Dec 2010

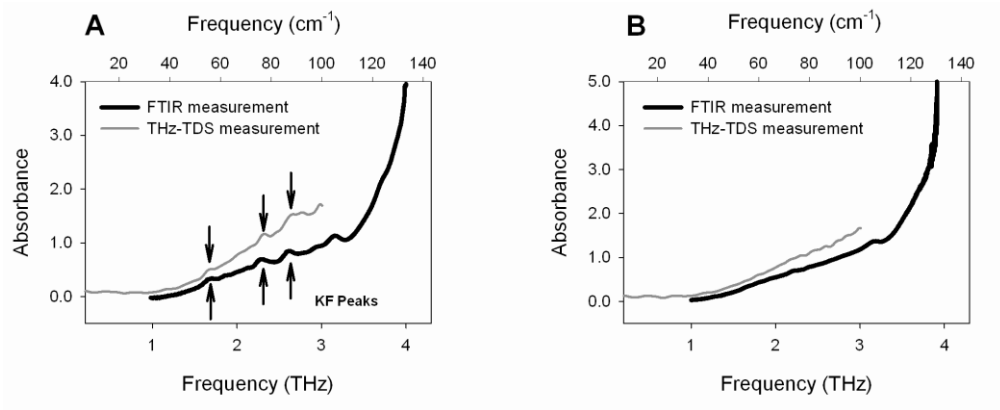


*Fig. 6* A comparison of absorption spectra from THz-TDS setup (grey) and FTIR setup (black). A) KF buffer. The arrows indicate the phonon-like resonance found in both measurements. B) 50 mM AK17 in KF buffer. Data were collected at 80 K.

Prior to this study the absorption spectra of dried homopolymer peptides have been studied using FTIR with a synchrotron light source. A monotonic increase in absorbance with increasing frequency between 1.8 and 10.5 THz has been observed [28]. Other THz-TDS studies of hen egg white lysozyme prepared as concentrated aqueous samples also demonstrated a monotonic increase in absorbance with increasing frequency 0.2-2 THz at a temperature range of 160-250 K [14]. In our research we were able to measure spectra of peptides in an aqueous environment from 0.1 to up to 4 THz. We observed that the absorption of the peptide molecules was higher than water absorbance at 79 K and that a monotonic increase in absorbance with increasing frequency and increasing peptide concentration was observable.

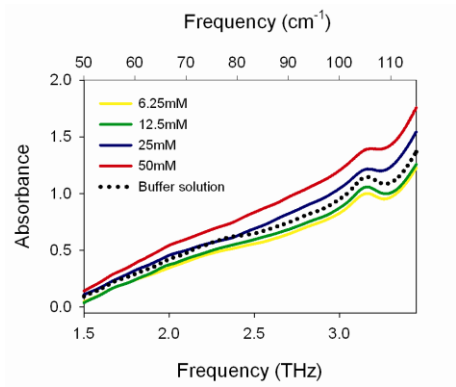


Fig. 7. The FTIR measurement of AK 17 peptide dissolved in 10 mM phosphate buffer, measured at 79 K. Red: 50 mM AK17, Blue: 25 mM AK17, Green: 12.5 mM AK17, Yellow: 6.25 mM AK17, black dot: buffer.

For both THz-TDS and FTIR measurements, absorbance initially dropped as the concentration of the peptide was increased (to 12.5 mM). This can be explained with regard to the population of biological water. It is known that ice crystal formation is suppressed next to the surface of biomolecules as the water in the solvation shell remains liquid as the bulk water freezes [29]. A recent study of the solvation shell around proteins suggested that a fragile (high density liquid) to strong (low density liquid) transition occurs at approximately 220 K [14,30]. The solvation shell may form a low-density amorphous ice below 220 K, which leads to a lower absorption compared to the crystalline ice formed from bulk water and likely accounts for the drop in absorbance we observe at low peptide concentrations, as shown in

#137135 - $15.00 USD Received 27 Oct 2010; revised 8 Dec 2010; accepted 8 Dec 2010; published 14 Dec 2010

Fig. 5. At higher peptide concentrations, the solvation shells may overlap as described in section 3.1, the influence of solvation shell on the overall absorbance plateau and peptide dynamics are a major driving force for the monotonic increase in absorbance with increasing peptide concentration. These data indicate that it is feasible to analyze the absorbance of peptides in ice at low temperature. Structural-specific changes in absorbance could not be observed among the three peptides under investigation. This is in contradiction to the low temperature absorption measurements of native and denatured egg white lysozyme [14]. It should be noted that the role of the solvation shell has to be considered even at low temperatures, although its dimensions in the frozen state are not known.

*3.3 Applicability of THz-TDS to study low temperature liquid samples*

Biological samples often contain a high level of ionic components such as salts or small molecular weight organic molecules. As mentioned in section 3.2, salt crystal formation resulting from the freezing process can introduce unwanted effects in absorbance spectra. For this reason, we further investigate the mechanism of salt crystal formation, as well as the peptide-related inhibitory effects using the synchrotron FTIR setup. In addition to the three positively charged peptides (AK17, AK10G and AK9P), a neutral peptide AQ17 was also synthesized and tested. Four solute concentrations (3.125 mM, 6.25 mM, 12.5 mM and 25 mM) were examined for all four peptides and the peak height of the strongest KF dihydrate phonon-like resonance peak in our spectral range at 2.64 THz was quantified. The results shown in Fig. 8 demonstrate a progressive extinction of the KF crystal peak resonance with increasing peptide concentration.

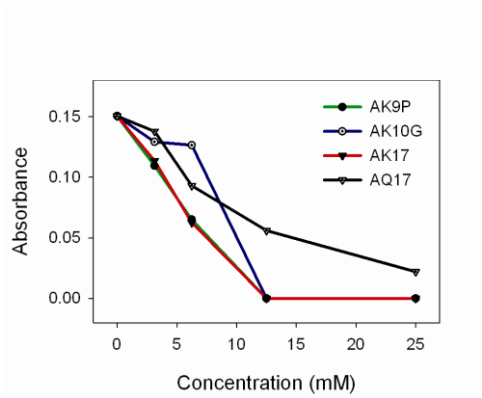


Fig. 8. The effect of different concentration of peptide on the salt crystallization. Data points are collected from FTIR measurements at 79 K. Peak height at 87 $cm^{-1}$ is extracted against the absorption baseline and plotted against the peptide concentrations. Red: AK17, Blue: AK10G, Green: AK9P and Black: AQ17.

It has previously been demonstrated that THz-TDS is capable of detecting subtle crystal transformations in the solid state [31–33]. From a method development perspective, the existence of inorganic crystals in association with certain buffer is of great importance. This phenomenon is largely driven by the relationship between salt solubility and temperature. When 0.1 M of KF buffer was frozen in liquid nitrogen, ice crystals started to form at temperatures above the eutectic point of KF. The KF ions were concentrated into the unfrozen liquid between the growing ice crystals, reaching super-saturation where homogeneous nucleation could proceed. In all of our measurements, it was evident that the formation of KF crystals was disrupted by the presence of the four different 17 amino acid peptide molecules. We observed a very similar concentration-dependence of the inhibition with all four peptides tested. The three charged lysine-containing peptides (AK17, AK10G and AK9P) exhibited similar profiles in inhibiting KF crystal formation. The secondary structure difference among

#137135 - $15.00 USD Received 27 Oct 2010; revised 8 Dec 2010; accepted 8 Dec 2010; published 14 Dec 2010

the three lysine-containing peptides did not affect the profile significantly, suggesting the peptide-KF interaction was not peptide structure-specific. In contrast, the weaker salt-crystal inhibition displayed by the uncharged peptide (AQ17) suggested a probable role of electrostatic interactions in this process. It is intrinsically difficult to separate the inhibition of nucleation from that of crystal growth. Other techniques, for example synchrotron X-ray diffraction [34], are required to complement the results observed by vibrational spectroscopy. According to studies of the Hofmeister series [35], fluoride ions typically only interact indirectly with biomolecules via intervening water molecules. Therefore, the presence of 12.5 mM net positive ( + 4) charged peptides will not dramatically lower the availability of fluoride ion in free solution and thus is not likely to be the main driving force in reducing crystallization. A measurement was also performed on a 0.05 mM KF solution and crystal signals were detected in the resulting spectrum (data not shown). On the basis of a progressive inhibition effect observed in all peptides, this phenomenon could be explained in the context of crystal growth. In an early study on a biogenic crystal [36] it has been proposed that an interfacial reaction, rather than transportation of the ion, is the rate controlling mechanism of crystal growth. More specifically, inhibitors of crystallization block the free access of constituent ions by adsorption at the crystal-solution interface. Although speculative, the difference in the crystal inhibition capability between charged and neutral peptides could be due to the variation in electrostatic complementarity with the KF crystal growing faces, while polypeptide-interfacial properties also play an important role.

Sample preparation is important when undertaking analysis of biological samples in the THz and far infrared part of the spectrum [37]. Phonon-like resonances due to salt crystal formation in biological samples can be misinterpreted as features associated with the molecule being studied. In many cases this can be overcome by careful choice of buffer. If sample preparation issues are resolved THz-TDS has the potential to be a powerful and sensitive technique for studying absorbance of biological materials in the THz part of the spectrum at low temperature where water absorbance is reduced.

## 4. Conclusion

The usefulness of analysis of peptide solutions using THz-TDS at room temperature was restricted by the relatively high absorbance of water compared to the peptide. Analysis of peptide samples in an aqueous environment at room temperature did not enable measurement of the peptide's absorbance. Freezing of the sample radically reduced absorbance due to water but introduced additional considerations. Distinct phonon resonances for the peptides studied here were not detected, even though the peptides had very different secondary structure. Overall absorbance of a peptide solution is, however, sensitive to peptide concentration as this affects both the excluded volume of solvent and extent of overlap of solvations shells. THz-TDS and FTIR appear to be able to probe both of these aspects of solvated biomolecules. Most aqueous environments include salts and small organic molecules that can crystallize during freezing to produce discrete phonon-like resonances, allowing salt crystallization the presence of biomolecules to be studied. However, if detecting the absorbance spectrum between 0.1 and 3.0 THz (3.3-100 $cm^{-1}$) of the macromolecule is the desired outcome, the low molecular weight material has to be excluded from the sample. In this paper, the interaction between peptide and KF, and the effect on KF crystallization during freezing was studied. This approach may prove to be useful for researchers studying crystallization during lyophilization, a procedure important to the pharmaceutical industry, particularly given the apparent sensitivity to biological water.

## Acknowledgements

This work was funded by the Australian Research Council grant number DP0773111 and supported by the National Collaborative Research Infrastructure Strategy, an Australian Federal Government initiative. We thank the Australian Synchrotron for access to their

infrared beamline (grant numbers FI1137 and FI1437), and Dominique Appadoo and Danielle Martin of the Australian Synchrotron for their assistance. TD thanks the University of Queensland for an international travel grant. JAZ thanks Gonville & Caius College, Cambridge for a Research Fellowship. RL thanks the EPSRC and Trinity College, Cambridge for funding his PhD.

#137135 - $15.00 USD Received 27 Oct 2010; revised 8 Dec 2010; accepted 8 Dec 2010; published 14 Dec 2010